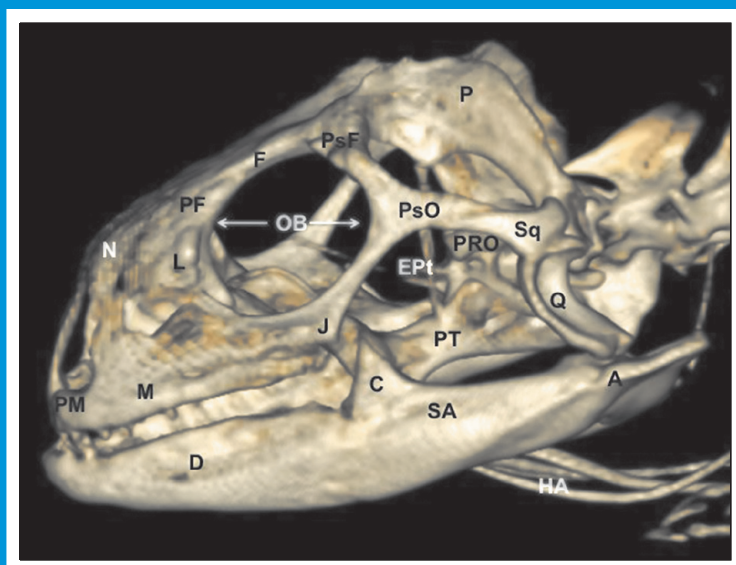


THE SCIENTIFIC JOURNAL OF THE VETERINARY FACULTY UNIVERSITY OF LJUBLJANA

SLOVENIAN VETERINARY RESEARCH

SLOVENSKI VETERINARSKI ZBORNIK



Volume
58 3

THE SCIENTIFIC JOURNAL OF THE VETERINARY FACULTY UNIVERSITY OF LJUBLJANA

SLOVENIAN VETERINARY RESEARCH

SLOVENSKI VETERINARSKI ZBORNIK

Volume
58 3

Slov Vet Res • Ljubljana • 2021 • Volume 58 • Number 3 • 91 – 120

The Scientific Journal of the Veterinary Faculty University of Ljubljana

SLOVENIAN VETERINARY RESEARCH SLOVENSKI VETERINARSKI ZBORNIK

Previously: RESEARCH REPORTS OF THE VETERINARY FACULTY UNIVERSITY OF LJUBLJANA
Prej: ZBORNIK VETERINARSKE FAKULTETE UNIVERZA V LJUBLJANI

4 issues per year / izhaja štirikrat letno
Volume 58, Number 3 / Letnik 58, Številka 3

Editor in Chief / glavni in odgovorni urednik: Gregor Majdič
Co-Editor / sourednik: Modest Vengušt
Technical Editor / tehnični urednik: Matjaž Uršič
Assistants to Editor / pomočnici urednika: Valentina Kubale Dvojmoč, Klementina Fon Tacer

Published by / Založila: University of Ljubljana Press / Založba Univerze v Ljubljani
For the Publisher / Za založbo: Igor Papič, the Rector of the University of Ljubljana / rektor Univerze v Ljubljani

Issued by / Izdala: Veterinary Faculty University of Ljubljana / Veterinarska fakulteta Univerze v Ljubljani
For the Issuer / Za izdajatelja: Andrej Kirbiš, the Dean of the Veterinary Faculty / dekan Veterinarske fakultete

Editorial Board / uredniški odbor:

Vesna Cerkvenik, Robert Frangež, Polona Juntos, Tina Kotnik, Matjaž Ocepek, Ožbalt Podpečan, Ivan Toplak, Milka Vrecl, Veterinary Faculty University of Ljubljana / Veterinarska fakulteta Univerze v Ljubljani ; Simon Horvat, Janez Salobir, Biotechnical Faculty University of Ljubljana / Biotehniška fakulteta Univerze v Ljubljani; Andraž Stožer, Faculty of Medicine University of Maribor / Medicinska fakulteta Univerze v Mariboru

Editorial Advisers / svetovalca uredniškega odbora: Gita Grecs-Smole for Bibliography (bibliotekarka),
Leon Ščuka for Statistics (za statistiko)

Reviewing Editorial Board / ocenjevalni uredniški odbor:

Antonio Cruz, Institute Suisse du Medicine Equine (ISME), Vetsuisse Fakultät, University of Bern, Switzerland; Gerry M. Dorrestein, Dutch Research Institute for Birds and Exotic Animals, Veldhoven, The Netherlands; Sara Galac, Utrecht University, The Netherlands; Wolfgang Henninger, Veterinärmedizinische Universität Wien, Austria; Nevenka Kožuh Eržen, Krka, d.d., Novo mesto, Slovenia; Louis Lefaucheur, INRA, Rennes, France; Peter O'Shaughnessy, Institute of Comparative Medicine, Faculty of Veterinary Medicine, University of Glasgow, Scotland, UK; Peter Popelka, University of Veterinary Medicine, Košice, Slovakia; Dethlef Rath, Institut für Tierzucht, Forschungsbericht Biotechnologie, Bundesforschungsanstalt für Landwirtschaft (FAL), Neustadt, Germany; Phil Rogers, Grange Research Centre, Dunsany, Co. Meath, Ireland, Ireland; Alex Seguino, University of Edinburgh, Scotland, UK; Henry Staempfli, Large Animal Medicine, Department of Clinical Studies, Ontario Veterinary College, Guelph, Ontario, Canada; Frank J. M. Verstraete, University of California Davis, Davis, California, US; Thomas Wittek, Veterinärmedizinische Universität, Wien, Austria

Address: Veterinary Faculty, Gerbičeva 60, 1000 Ljubljana, Slovenia
Naslov: Veterinarska fakulteta, Gerbičeva 60, 1000 Ljubljana, Slovenija
Tel.: +386 (0)1 47 79 100, Fax: +386 (0)1 28 32 243
E-mail: slovetres@vf.uni-lj.si

Sponsored by the Slovenian Research Agency
Sofinancira: Javna agencija za raziskovalno dejavnost Republike Slovenije

ISSN 1580-4003

Printed by/tisk: DZS, d.d., Ljubljana, September 2021

Number of copies printed / Naklada: 220

Indexed in/indeksirano v: Agris, Biomedicina Slovenica, CAB Abstracts, IVSI
Ulrich's International Periodicals Directory, Science Citation Index Expanded,
Journal Citation Reports – Science Edition
<https://www.slovetres.si/>

This work is licensed under a Creative Commons Attribution-ShareAlike 4.0 International License / To delo je ponujeno pod licenco
Creative Commons Priznanje avtorstva-Deljenje pod enakimi pogoji 4.0 Mednarodna licenca

SLOVENIAN VETERINARY RESEARCH SLOVENSKI VETERINARSKI ZBORNIK

Slov Vet Res 2021; 58 (3)

Original Research Articles

- Kandeel M, El-Deeb W, Fayed M, Ghoneim I. Pharmacokinetics of the long-acting ceftiofur crystalline-free acid in Arabian she-camels (*Camelus dromedarius*) 95
- Strašek Smrdel K, Avšič T. The detection of *Anaplasma phagocytophilum* and *Babesia vulpes* in spleen samples of red fox (*Vulpes vulpes*) in Slovenia 103
- Pérez S, Encinosa M, Morales M, Arencibia A, Suárez-Bonnet A, González-Rodríguez E, Jaber JR. Comparative evaluation of the Komodo dragon (*Varanus komodoensis*) and the Green iguana (*Iguana iguana*) skull by three-dimensional computed tomographic reconstruction 111

Case Report

- Garcês A, Soeiro V, Lóio S, Silva F, Pires I. Osteomyelitis on the cervical vertebrae of a free-living European hedgehog (*Erinaceus europaeus*) by *Paeniclostridium sordellii* 117
-

PHARMACOKINETICS OF THE LONG-ACTING CEFTIOFUR CRYSTALLINE-FREE ACID IN ARABIAN SHE-CAMELS (*Camelus Dromedarius*)

Mahmoud Kandeel^{1,2}, Wael El-Deeb^{3*,4}, Mahmoud Fayez⁵, Ibrahim Ghoneim³

¹Department of Biomedical Sciences, ³Department of Clinical Sciences, College of Veterinary Medicine, King Faisal University, Al-Ahsa, 31982, Saudi Arabia, ²Department of Pharmacology, Faculty of Veterinary Medicine, Kafrelshikh University, Kafrelshikh, 35255, ⁴Department of Internal Medicine, Infectious Diseases and Fish Diseases, Faculty of Veterinary Medicine, Mansoura University, Mansoura, Egypt, ⁵Veterinary Serum and Vaccine Research Institute, Cairo, Egypt

*Corresponding author, E-mail: weldeeb@kfu.edu.sa

Abstract: Ceftiofur is an important broad-spectrum 3rd generation cephalosporin antibiotic. Owing to its time-dependent antimicrobial actions, the length of time of being above bacterial MIC is the critical point in using ceftiofur for chemotherapy rather than its peak of concentration. Consequently, this experiment was carried out to evaluate, for the first time, the pharmacokinetics of the long-acting ceftiofur crystalline acid-free form (ceftiofur-CAF) in camels. Ceftiofur-CAF 200 mg/ml suspension sterile solution was injected i/m at a dose 6.6 mg/kg. Blood samples were collected from the jugular vein in vacutainer tubes at 0, 0.13, 0.25, 0.5, 1, 2, 4, 8, 12, 24, 48, 72, 96, 120, and 144 hours after administration of the drug. Ultrahigh Performance Liquid Chromatography-Mass Spectrometry (UPLC MS/MS) was used to measure serum concentration. Pharmacokinetic modeling was by a two-compartment model. Pharmacokinetics of ceftiofur-CAF after single i/m injection in she-camels was best modeled in the two-compartment model, where the drug slowly distributed to a second compartment with poor tissue penetration and high preference to the central compartment. In this study, the maximum plasma concentration (C_{max}) was $9.29 \pm 0.42 \mu\text{g/ml}$ at T_{max} equals 9.41 ± 1.35 h. The area under the curve ($AUC_{0-\infty}$) was $354.1 \pm 57.22 \mu\text{g/ml} \cdot \text{h}$. The distribution and elimination half-lives were 7.42 and 46.13 h, respectively. The mean residence time (MRT) was 42.01 h. Compared with the rapidly absorbed form of ceftiofur (ceftiofur-RAF) in camels, there was almost similar maximal serum concentration but with delayed time to maximal concentration (T_{max}), longer means residence time (MRT) and higher distribution and elimination half-lives. In terms of antibacterial efficacy, ceftiofur-CAF stayed above a previously recommended level of 0.2 $\mu\text{g/ml}$ for 7 days, which can be achieved after a single i/m injection of 6.6 mg/kg. The obtained pharmacokinetics data in camels recommends repeated administration of 2 days apart for bacteria requiring MIC levels above 2 $\mu\text{g/ml}$.

Key words: Ceftiofur; pharmacokinetics; camel; cephalosporins

Introduction

Ceftiofur is a semisynthetic 3rd generation cephalosporin with broad-spectrum antibacterial efficiency by inhibition of essential enzymes in cell wall biosynthesis resulting in a strong bactericidal effect (1, 2). It has been approved for veterinary medical uses in various animal species including equines, bovines, swine, sheep, and goats (3). The crystalline-free acid form of ceftiofur at a dose

rate of 6.6 mg/kg can be used in two consecutive injections to cover a treatment course of 10 days (1). This is more beneficial than the laborious single daily dosing strategy.

Recently, camels have been reported to acquire serious respiratory infections caused by various bacterial and viral causative agents as middle east respiratory syndrome coronavirus (MERS CoV) or bacterial pneumonia (4, 5). Owing to the emerging nature of camel pathogens and their public health impact, proper therapeutic protocols have to be achieved.

Ceftiofur is an excellent choice in treating respiratory infections in horses, cattle, and swine (1).

The usage of a long-acting formula of ceftiofur is thought to deliver significant-high serum concentration of ceftiofur for at least 4 days after a single i/m injection in horses and other animals (1, 3, 6-9). This will be beneficial in creating antimicrobial coverage in treating camel pathogens and during mass treatment of respiratory infections in camels. Moreover, a single long-acting dose minimizes handling and avoid stresses on camels during restraining and repeated daily injections. Despite the availability of such long-acting ceftiofur preparation, its pharmacokinetics and drug disposition parameters in camels is not well understood. This study investigates for the first time the pharmacokinetics of ceftiofur crystalline acid-free form (Ceftiofur-CAF) in Arabian she-camels. The obtained pharmacokinetic parameters were compared with that of the previously published results of ceftiofur immediate-release form (ceftiofur-IRF) in camels. This study will aid in designing dose frequencies and the proper design of antibacterial programs.

Materials and methods

Animals, facilities, and instruments

Three Arabian non-lactating 8 years old she-camels were used in this study. The she-camels were housed in the facilities of the camel research center, King Faisal University. Camels did not receive any previous treatments at least three months before the start of the experiment. Water was freely available during all experimental courses. She-camels were fed on alfalfa hay according to the camel center feeding schemes. The ethics committee of King Faisal University (no. 1811013) approved all experimental procedures and animal experiments. Waters Acquity Ultra-high performance liquid chromatography Mass-mass (UPLC-MS-MS) system equipped with an autosampler, C18 column, and Acquity Micromass triple-quadrupole was used to measure the serum concentration of injected Ceftiofur.

Drug administration

Ceftiofur-CAF 200 mg/ml suspension (Excede, Zoetis Inc, NJ, USA) sterile solution was injected i/m at a dose 6.6 mg/kg.

Collection of samples

Blood samples were collected from the left jugular vein in vacutainer tubes at 0, 0.13, 0.25, 0.5, 1, 2, 4, 8, 12, 24, 48, 72, 96, 120, and 144 hours after administration of the drug Administration. Blood samples were inverted briefly for three times and kept in insulated refrigerated boxes to clot. After 15 min, the tubes were centrifuged at room temperature at 2000 g for 15 min. Aliquots of serum were stored at - 80 °C until chromatographic analysis.

Sample preparation and extraction

The sample preparation was performed as described by (10, 11) with slight variations. A standard stock solution at different concentrations was prepared by dilution in MilliQ water starting from 150 to 3.125 ng/ml concentrations. Within this range, six different concentrations were used to plot the standard curve. All tubes were stored at - 30°C and melted just before the experiment.

Sample preparation included deproteinization, evaporation of the solvent, and final dissolving of the mobile phase. Serum was deproteinized in acetonitrile 1:7 (v/v). After vortexing, the denatured protein was removed by centrifugation for 13,000 rpm for 10 min. the supernatant was evaporated under a nitrogen stream and the pellet was redissolved in the mobile phase. Twenty microliters of the solution were injected into the UPLC-MS-MS system.

Chromatographic conditions

UPLC-MS/MS was performed using a Waters Acquity UPLC system (Waters Corp., MA, USA). The system is composed of Waters Acquity Micromass triple-quadrupole MS quadrupole with electrospray source, Waters Acquity BEH C18 column, autosampler, quaternary solvent management system. The system was operated under the control of MassLynx 4.1 software. The mass multi-reaction-monitoring (MRM) mode was as described previously (10, 12, 13). The running solution contained solution (A): UPLC grade water containing 0.1% formic acid, and solution (B): methanol containing 0.1% formic acid. Half mM ammonium acetate was added for both solutions A and B. The gradient elution program (14) comprised a gradual increase in

solution B until 85:15 (v/v). validations of runs and limits of detection quantification were performed as described previously (15). The method was validated for selectivity, sensitivity, linearity, precision, accuracy, and stability. The blank and drug samples were compared to assign the chromatographic selectivity. LLOQ (lower limit of quantification) was used as a measure of sensitivity by measuring the area of the curve that was at least five times higher than the blank values. Drug concentrations of 0.195 ppb to 150 ppb were used for linearity checking. Intra and inter-day precision was carried out by measuring LLOQ, LOC, middle-quality control (MQC), and high-quality control (HQC) levels. Accuracy was assigned by estimation of the amount extracted after the addition of known amounts of the drug. The chromatograms for LOD and LOQ are given in the supplementary materials (Supplementary files 1 and 2).

Pharmacokinetic analysis

The pharmacokinetic analysis was performed by nonlinear curve fitting analysis. The data were fitted with the aid of PKsolver Excel add-on software (16).

Results

Both non-compartment and compartment pharmacokinetic models were used to fit the obtained data. Fig.1 shows the relation between the serum concentrations of ceftiofur-CAF concerning time. The best-fitting was determined to be by a two-compartment model to deliver the pharmacokinetic parameters (Table 1): α and β : the apparent rate constants of the distribution and elimination phases, the distribution and elimination half-lives ($t_{1/2\alpha}$ and $t_{1/2\beta}$), the rate constant for equilibration between the central and peripheral compartment (k_{12}), return to the central compartment (k_{21}), elimination from central component (k_{10}) and the volume of distribution (V_F). The rate constant for distribution to the peripheral compartment was 0.03 h^{-1} indicating slow transfer of drug from the central to peripheral compartment. The values of k_{12} and k_{21} indicate low and slow tissue penetration and a general preference for central compartment or serum. The area under the concentration curve ($AUC_{0-\infty}$) was $354.1 \mu\text{g/ml h}^{-1}$ and mean residence time (MRT) 42.01 h.

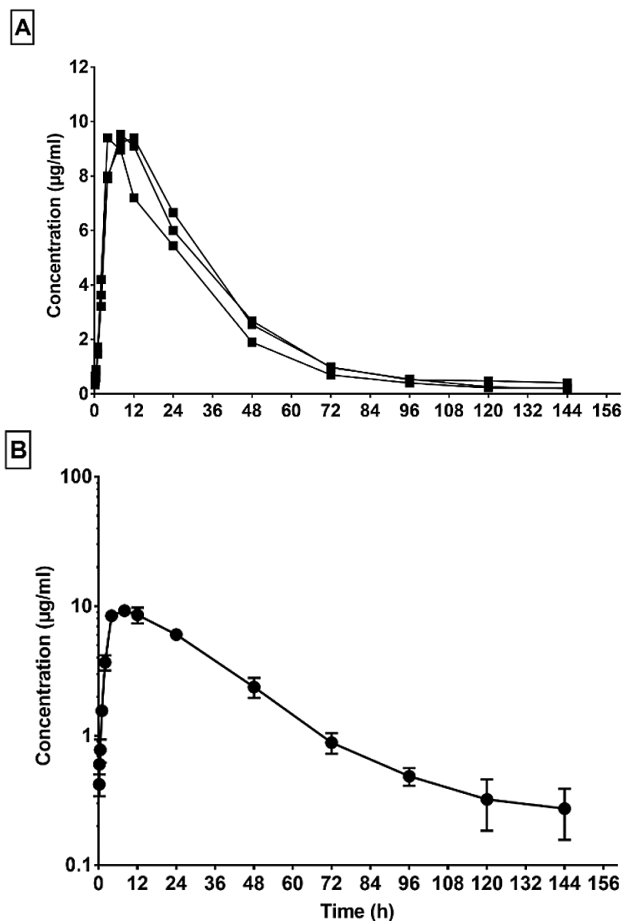


Figure 1: The relation between the serum concentrations of ceftiofur-CAF concerning time. A) the concentration (Y-axis) is plotted against time (X-axis). The values of each she-camel are plotted separately. B) semi-logarithmic plot of concentration-time relation. The values represent mean \pm SD

Table 1: Pharmacokinetic parameters of single i/m injection of 6.6 mg/kg of ceftiofur-CAF in she-camels (n = 3)

| Parameter | Unit | Average | SD |
|----------------------|-------------------|---------|--------|
| A | µg/ml | 140.89 | 109.01 |
| α | 1/h | 0.11 | 0.05 |
| B | µg/ml | 5.77 | 4.39 |
| β | 1/h | 0.02 | 0.01 |
| ka | 1/h | 0.15 | 0.02 |
| Parameter | Unit | Average | SD |
| k ₁₀ | 1/h | 0.05 | 0.01 |
| k ₁₂ | 1/h | 0.03 | 0.02 |
| k ₂₁ | 1/h | 0.05 | 0.04 |
| t _{1/2α} | h | 7.42 | 4.24 |
| t _{1/2β} | h | 46.13 | 37.75 |
| t _{1/2ka} | h | 4.64 | 0.75 |
| V/F | (mg/kg)/(µg/ml) | 0.35 | 0.04 |
| CL/F | (mg/kg)/(µg/ml)/h | 0.02 | 0.001 |
| V ₂ /F | (mg/kg)/(µg/ml) | 0.29 | 0.15 |
| CL ₂ /F | (mg/kg)/(µg/ml)/h | 0.01 | 0.01 |
| T _{max} | h | 9.41 | 1.35 |
| C _{max} | µg/ml | 9.29 | 0.42 |
| AUC _{0-t} | µg/ml*h | 335.55 | 36.25 |
| AUC _{0-inf} | µg/ml*h | 354.10 | 57.22 |
| MRT | h | 42.01 | 15.64 |

Discussion

This study investigated the pharmacokinetics of ceftiofur long-acting preparation in camels. This will help in the design of a suitable dosing program. Hibbard et al. (2002) reported that a single s/c injection of ceftiofur-CAF produced plasma levels of ceftiofur remained above 0.2 µg/ml for more than 7 days (7). In this study, ceftiofur-CAF injection in camels resulted in slow absorption from the injection site to reach a C_{max} and T_{max} of 9.41 µg/ml and 9.29 hours, respectively (Table 1). This indicates about 8 folds increase in the absorption time from the i/m injection site compared with immediate-release ceftiofur in camels, which was 1.22 h (17). Additionally, the C_{max} of ceftiofur-CAF was 9.29, which is highly comparable to the previously reported C_{max} of ceftiofur-IRF, 10.34 µg/ml (17).

The obtained C_{max} in she-camels (9.29 µg/ml) was prominently higher than 2.248 µg/ml in nonlactating goats (6), 1.458 in lactating goats (6), 6.39 µg/ml in beef cattle (6), 4.44 µg/ml in

dairy cow, 2.45 µg/ml in sheep and 0.785 µg/ml in equine (1). The s/c injection in dairy cows, sheep, and goats, compared with i/m injection in this study might affect the peak of serum concentration. However, the several folds higher serum concentration in camels suggests the delayed absorption and camel specific factors in ceftiofur disposition. The obtained T_{max} in she-camels (9.41 h) is to be described as an earlier peak of ceftiofur concentration compared with 26.67 h in nonlactating goats (6) 46 h in lactating goats (6), 23 h in sheep (18), and 22 h in equine (1). The absorption half-life (t_{1/2βka}) of ceftiofur-CAF in she-camels was 4.64 h, this is lower than the estimated value of 5.67 in nonlactating goats (6).

The distribution half-life (t_{1/2α}) was 7.42 h indicating slow distribution. The t_{1/2α} obtained in ceftiofur-IRF was recording less than 1 h in cattle, sheep, and goats and about 0.34 h in camels (17). Similarly, the estimated elimination half-life (t_{1/2β}) was 46.13 h that is greatly higher than the average recorded value for ceftiofur-IRF, which was in the range of 3.18-5.83 h in cattle,

sheep, calves, or goats (17). Thus, ceftiofur-CAF produced a prominent long-lasting slow-release form in camels by showing delayed T_{max} and longer distribution and elimination half-lives. The elimination half-life ($t_{1/2\beta}$) of ceftiofur-CAF in she-camels was 46.13 h, which is more or less similar to 47.31 h in nonlactating goats (6) and 100 h in equine (1). This implies species-specific differences in $t_{1/2\beta}$ in animal species. The administration of ceftiofur-IRF in domestic and exotic birds showed wide variability in pharmacokinetic parameters with $T_{max} = 0.83$ - 2.67 h, $C_{max} = 0.86$ - 10.99 $\mu\text{g/ml}$, $t_{1/2\alpha} = 0.28$ - 3.8 h and $t_{1/2\beta} = 2.5$ - 8.65 h (19). This indicates the wide variability of ceftiofur pharmacokinetics.

The model for fitting ceftiofur-CAF pharmacokinetics was best explained by using a non-compartmental model in neonatal foals (3), equine (1), cattle egrets (9), guinea fowl (20), American flamingos (21), ball python (22), and Rhesus macaques (8), one-compartment model in sheep (18) and goat (6) and two-compartment model in swine (23). The present data were fitted by a two-compartment model. This model was used to fit the pharmacokinetics data in pigs injected with commercial ceftiofur HCl suspension at a dose rate of 5 mg/kg (23). Compared with pigs data, she-camels pharmacokinetic parameters showed a 6-folds increase in distribution half-life, 10.45-folds increase in absorption half-life, 5.9-folds increase in T_{max} , 3.8 times lower C_{max} , and 3.36-folds increase in elimination half-life. This indicates delayed absorption, distribution, and elimination time in camels. Additionally, the drug levels fall below the recommended level of 0.2 $\mu\text{g/ml}$ in pigs in less than 96 h, compared with 144 h in camels.

The analysis of the relation between the drug concentration and bacterial susceptibility was based on MIC levels for susceptible respiratory pathogens in cattle (7, 17). The obtained pharmacokinetic parameters revealed that one dose of i/m injection of ceftiofur-CAF at a dose rate of 6.6 mg/kg achieved serum levels above 0.2 $\mu\text{g/ml}$ for 7 days in she-camels. In our study, the concentration of ceftiofur remained above 0.2 $\mu\text{g/ml}$ for an average time of 119.833 h. Moreover, for proper antibacterial efficiency, achieving serum concentrations about 10-times the MIC values (24) or a serum level of 2 $\mu\text{g/ml}$ is required. Based on pharmacokinetic parameters, the level of ceftiofur falls below 2 $\mu\text{g/ml}$ after 48 h of injection. Therefore, a single injection is sufficient to cover 7 days for highly susceptible

bacteria and it is recommended to administer a second dose of ceftiofur-CAF after 2 days from the first injection for less susceptible bacteria. The estimated ceftiofur levels were above 0.2 $\mu\text{g/ml}$ for 9.1 days in beef cattle (6.6 mg/kg), 6.7 days in nonlactating goats, 8.5 days in dairy cows, and 7.5 days in lactating goats (6). This indicates a shorter duration in she-camels compared with other animals. Taking into consideration the "flip-flop" pharmacokinetics of slow-release preparations, the terminal phase of elimination of the drug is complicated by its slow release from the injection site. However, the impact of "flip-flop" pharmacokinetics is underscored in this camel experiment, as the half-life of absorption (4.64 h) is much lower than the elimination half-life ($t_{1/2\beta}$).

Conclusion: Ceftiofur-CAF achieved long-lasting serum levels in camels above the recommended level of 0.2 $\mu\text{g/ml}$ for 4 days following a single i/m injection at a dose rate of 6.6 mg/kg. Careful dose adjustment depending on MIC values could be practiced by comparing its value with the provided concentration-time relation. Camels showed a higher peak of serum concentration with markers of slow excretion and longer persistence in the body compared with other animals.

Acknowledgments

The authors would like to acknowledge the Deanship of Scientific Research at King Faisal University for their financial support under the research group support track (grant no. 1811013).

The authors declare that they have no conflict of interest.

All animals' procedures were approved by the ethics committee of King Faisal University (approval no: 1811013). Informed consent not apply to this work.

Authors' contributions, MK, WE, and MF designed the experiment, MK, WE, MF, IG performed the experiment, MK, WE, MF analyzed the results, MK, WE, and MF wrote the manuscript, MK, WE, MF, IG approved the submission.

References

1. Collard W, Cox S, Lesman S, et al. Pharmacokinetics of ceftiofur crystalline-free acid sterile suspension in the equine. *J Vet Pharmacol Ther* 2011; 34: 476-81.

2. Oliver S, Gillespie B, Headrick S, et al. Efficacy of extended ceftiofur intramammary therapy for the treatment of subclinical mastitis in lactating dairy cows. *J Dairy Sci* 2004; 87: 2393–400.
3. Hall T, Tell L, Wetzlich S, McCormick J, Fowler L, Pusterla N. Pharmacokinetics of ceftiofur sodium and ceftiofur crystalline free acid in neonatal foals. *J Vet Pharmacol Ther* 2011; 34: 403–9.
4. Al-Tarazi Y. Bacteriological and pathological study on pneumonia in the one-humped camel (*Camelus dromedarius*) in Jordan. *Rev Elevage Med* 2001; 54: 93–7.
5. Abbas B, Omer O. Review of infectious diseases of the camel. *Vet Bull* 2005; 75: 1–16.
6. Doré E, Angelos JA, Rowe JD, et al. Pharmacokinetics of ceftiofur crystalline free acid after single subcutaneous administration in lactating and nonlactating domestic goats (*Capra aegagrus hircus*). *J Vet Pharmacol Ther* 2011; 34: 25–30.
7. Hibbard B, Robb EJ, Chester JS, Dame KJ, Moseley WW, Bryson WL. Dose determination and confirmation for ceftiofur crystalline-free acid administered in the posterior aspect of the ear for control and treatment of bovine respiratory disease. *Vet Ther* 2002; 3: 22–30.
8. Salyards GW, Knych HK, Hill AE, Kelly KR, Christie KL. Pharmacokinetics of ceftiofur crystalline free acid in male rhesus macaques (*Macaca mulatta*) after subcutaneous administration. *J Am Assoc Lab Anim Sci* 2015; 54: 557–63.
9. Waldoch JA, Cox SK, Armstrong DL. Pharmacokinetics of a single intramuscular injection of long-acting ceftiofur crystalline-free acid in cattle egrets (*Bubulcus ibis*). *J Avian Med Surg* 2017; 31: 314–9.
10. Legrand T, Vodovar D, Tournier N, Khoumour N, Hulin A. Simultaneous determination of eight beta-lactam antibiotics, amoxicillin, cefazolin, cefepime, cefotaxime, ceftazidime, cloxacillin, oxacillin, and piperacillin, in human plasma by using ultra-high-performance liquid chromatography with ultraviolet detection. *Antimicrob Agents Chemother* 2016; 60: 4734–42.
11. Wang J, Fan X, Liu Y, et al. Extraction optimization of sixteen cephalosporins in milk by filtered solid-phase extraction and ultra high-pressure liquid chromatography coupled to tandem mass spectrometry. *Anal Methods* 2017; 9: 1282–9.
12. Hou XL, Wu YL, Lv Y, Xu XQ, Zhao J, Yang T. Development and validation of an ultra-high-performance liquid chromatography-tandem mass spectrometry method for determination of 10 cephalosporins and desacetylcefapirin in milk. *J Chromatogr B Anal Technol Biomed Life Sci* 2013; 931: 6–11.
13. Zaki AM, van Boheemen S, Bestebroer TM, Osterhaus AD, Fouchier RA. Isolation of a novel coronavirus from a man with pneumonia in Saudi Arabia. *N Engl J Med* 2012; 367: 1814–20.
14. Amatya R. Multi-class, multi residue method for determination of penicillins, cephalosporins, and quinolones in cow milk and validation in accordance with Commission Decision 2002/657/EC. Barcelona : University of Barcelona, 2010. (European Masters in Quality in Analytical Laboratories)
15. Shrivastava A, Gupta VB. Methods for the determination of limit of detection and limit of quantitation of the analytical methods. *Chron Young Sci* 2011; 2: 21.
16. Zhang Y, Huo M, Zhou J, Xie S. PKSolver: An add-in program for pharmacokinetic and pharmacodynamic data analysis in Microsoft Excel. *Comput Methods Programs Biomed* 2010; 99: 306–14.
17. Goudah A. Pharmacokinetics of ceftiofur after single intravenous and intramuscular administration in camels (*Camelus dromedarius*). *J Vet Pharmacol Ther* 2007; 30: 371–4.
18. Rivera-Garcia S, Angelos JA, Rowe JD, et al. Pharmacokinetics of ceftiofur crystalline-free acid following subcutaneous administration of a single dose to sheep. *Am J Vet Res* 2014; 75: 290–5.
19. Tell L, Harrenstien L, Wetzlich S, et al. Pharmacokinetics of ceftiofur sodium in exotic and domestic avian species. *J Vet Pharmacol Ther* 1998; 21: 85–91.
20. Wojick KB, Langan JN, Adkesson MJ, Cox SK, Gamble KC. Pharmacokinetics of long-acting ceftiofur crystalline-free acid in helmeted guineafowl (*Numida meleagris*) after a single intramuscular injection. *Am J Vet Res* 2011; 72: 1514–8.
21. Kilburn JJ, Cox SK, Backues KA. Pharmacokinetics of ceftiofur crystalline free acid, a long-acting cephalosporin, in American flamingos (*Phoenicopterus ruber*). *J Zoo Wildl Med* 2016; 47: 457–62.
22. Adkesson MJ, Fernandez-Varon E, Cox S, Martín-Jiménez T. Pharmacokinetics of a long-acting ceftiofur formulation (ceftiofur crystalline free acid) in the ball python (*Python regius*). *J Zoo Wildl Med* 2011; 42: 444–50.

23. Tang S, Xiao J, Guo G, He J, Hao Z, Xiao X. Preparation of a newly formulated long-acting ceftiofur hydrochloride suspension and evaluation of its pharmacokinetics in pigs. *J Vet Pharmacol Ther* 2010; 33: 238–45.

24. Quintiliani R. Pharmacodynamics of antimicrobial agents: time-dependent vs concentration-dependent killing. <http://www.antimicrobe.org/h04c.files/history/PK-PD%20Quint.asp> (March, 2021)

FARMAKOKINETIKA DOLGODELUJOČE CEFTIOFURNE KRISTALINIČNE PROSTE KISLINE PRI SAMICAH ARABSKIH KAMEL (*Camelus dromedarius*)

M. Kandeel, W. El-Deeb, M. Fayez, I. Ghoneim

Izveček: Ceftiofur je pomemben širokospektralni antibiotik 3. generacije cefalosporinov. Zaradi njegovih časovno odvisnih protimikrobnih učinkov je čas, ko je raven ceftiofura nad bakterijskim MIC in ne pri njegovem vrhu koncentracije kritična točka pri uporabi tega antibiotika. Poskus je bil izveden z namenom ovrednotenja farmakokinetike dolgo delujoče ceftiofurjeve kristalinične brezislinske oblike (ceftiofur-CAF) pri kamelah. Ceftiofur-CAF v koncentraciji 200 mg/ml suspenzije sterilne raztopine smo injicirali i/m v odmerku 6,6 mg/kg. Vzorci krvi so bili zbrani iz vratne vene v vakuumskih epruveh ob injiciranju antibiotika in nato 8, 15 in 30 minut po injiciranju ter 1, 2, 4, 8, 12, 24, 48, 72, 96, 120 in 144 ur po injiciranju antibiotika. Za merjenje serumske koncentracije je bila uporabljena tekočinska kromatografija ultra visoke ločljivosti (UPLC MS/MS). Farmakokinetično modeliranje je bilo izvedeno z dvokomponentnim modelom. Farmakokinetiko ceftiofur-CAF-a po enkratnem i/m injiciranju v kamele je bilo najbolje modelirati v modelu z dvema predelkoma, kjer se je zdravilo počasi razdeljevalo v drugi predelek s slabo penetracijo v tkiva in veliko prednostjo do osrednjega predelka. Najvišja koncentracija antibiotika v plazmi (C_{max}) je bila $9,29 \pm 0,42$ µg/ml pri T_{max} $9,41 \pm 1,35$ ure. Površina pod krivuljo ($AUC_{0-\infty}$) je bila $354,1 \pm 57,22$ µg/ml*h. Razpolovni čas razporeditve in izločanja je bil 7,42 oziroma 46,13 ure. Povprečni čas prisotnosti antibiotika (MRT) je bil 42,01 h. V primerjavi s hitro absorbirano obliko ceftiofurja (ceftiofur-RAF) pri kamelah je bila skoraj podobna največja koncentracija v serumu, vendar z zakasnjanim časom do največje koncentracije (T_{max}), daljšim časom zadrževanja (MRT) in večjim razpolovnim časom porazdelitve in izločanja. Ceftiofur-CAF ostal dni nad predhodno priporočeno ravni učinkovitosti 0,2 µg/ml kar 7 dni, kar je bilo mogoče doseči po enkratni i/m injekciji 6,6 mg/kg. Pridobljeni podatki o farmakokinetiki v kamelah priporočajo večkratno dajanje v razmaku 2 dni za bakterije, ki potrebujejo ravni MIC nad 2 µg/ml.

Ključne besede: Ceftiofur; farmakokinetika; kamela; cefalosporini

THE DETECTION OF *Anaplasma phagocytophilum* AND *Babesia vulpes* IN SPLEEN SAMPLES OF RED FOX (*Vulpes vulpes*) IN SLOVENIA

Katja Strašek Smrdel, Tatjana Avšič*

Institute of Microbiology and Immunology, Faculty of Medicine, Zaloška 4, 1000 Ljubljana

*Corresponding author, E-mail: tatjana.avsic@mf.uni-lj.si

Abstract: The entrance of wild animals into human settings serves as the access of vector-borne pathogens to susceptible hosts. A red fox (*Vulpes vulpes*) frequently enters and is quite adapted to living in urban and periurban environments. Due to its living habits, it could be a possible source of tick-borne pathogens, but it could also transfer pathogens through bites. One hundred and ten spleen samples from red foxes were screened for the presence of the *Anaplasma phagocytophilum* and *Babesia vulpes* genomes with real-time and conventional PCR. Positive PCR products were further sequenced. A genotype of *A. phagocytophilum* was determined and species of *Babesia* spp. if possible. Five (4.5%) spleen samples from red fox were positive for *A. phagocytophilum* DNA. With nucleotide comparison, three genotypes from cluster I were detected. The detected prevalence of *B. vulpes* in red fox in Slovenia was 76.3%. The parasite was detected in all tested regions of the country. Data from our study suggest that the red fox may have only limited impact on the circulation of the zoonotic genotype of *A. phagocytophilum*, but it represents a risk of transmission of *B. vulpes* near human settings and consequently poses a threat to domestic animals.

Key words: red fox, *Vulpes vulpes*; *Anaplasma phagocytophilum*; *Babesia* spp.; *Babesia vulpes*; tick-borne pathogens; dogs

Introduction

Wild carnivores, often in contact with domestic carnivores, are considered the primary source of tick-borne pathogens to humans (1). As the human population grows, urban areas expand and, consequently, more and different animal species enter human habitats (2). The red fox (*Vulpes vulpes*) represents the most widely distributed species in the order Carnivora. It is present across the Northern Hemisphere, that is Northern America, Europe, Asia and some parts of Africa (3). The red fox lives in distinct ecosystems

and frequently enters human settings. It has adapted to the urban environment mainly due to the availability of food and lack of predators (1). Recently, it has been recognized as a potential reservoir of several vector-borne pathogens and, therefore, a source of infection for domestic and companion animals and humans (3). It represents a sentinel species for *Anaplasma phagocytophilum* (4, 5), *Babesia* spp. (3, 6), *Bartonella* spp. (7) and many other vector-borne pathogens (3). Due to its natural environment, it is frequently exposed to different arthropod vectors (2) and to a non-vector-borne transmission of pathogens through bites.

A. phagocytophilum is a well-known tick-borne pathogen that infects humans and animals. Many ecotypes of *A. phagocytophilum* exist in nature, but

not all are pathogenic for humans and companion animals (8). Sequences of *A. phagocytophilum* isolated from red foxes belong to ecotype I, and some genotypes in this cluster are zoonotic (9). In Slovenia, in wild and domestic animals, several genotypes have been detected that belong to three ecotypes (10). It has been suggested that wild boar (*Sus scrofa*) could serve as reservoir species for a genotype that infects humans and dogs in Slovenia (11), but this animal rarely enters human environments. In contrast, during the night time, the red fox frequently searches for easily available food.

Babesiae are parasitic intracellular microorganisms that infect erythrocytes. They are transmitted by hard ticks and represent an increasing global risk to both animals and humans (12). *Babesia* spp. parasites are present in the Slovenian area, in dogs, small mammals, and cervids (13-15). Recently, a new babesial pathogen of dogs and red foxes has been recognized elsewhere; it belongs to the group *Babesia microti* (small babesiae like) (16). It is reported under various names: *Theileria (Babesia) annae*, *Babesia* sp. 'Spanish dog' isolate, *Babesia microti*-like, *Babesia* cf. *microti*; so far no current valid name is agreed upon (17). As red foxes from distant regions are highly infected with this parasite, it is suspected that fox is a natural host for this parasite, and the name *Babesia vulpes* was proposed (18). Infections with the parasite cause anaemia, thrombocytopenia, and azotemia in dogs (18), although asymptomatic infection has been reported, too (19). Foxes usually have no apparent clinical signs of the disease (18). As the red fox is quite adapted to urban and periurban areas, it poses a risk of transmission of the infection to domesticated dogs.

Wild carnivores are rarely examined for vector-borne pathogens, although they are highly infested with ticks and fleas. Adding the factors of global warming, deforestation, urbanization, human outdoor activities, etc. to improved molecular and diagnostic tools more new, emergent and re-emergent vector-borne pathogens are detected. Therefore, wild animals represent an important source of zoonotic agents. Our study aimed to detect the presence of selected pathogens in Slovenian population of red foxes.

Materials and methods

One hundred and ten red foxes (*V. vulpes*) of both sexes were shot by professional hunters during regular hunting season from autumn 1996 to spring 2003 (Table 1). From each animal, a sample of spleen was collected by hunters and delivered to our laboratory. Samples were stored at -20°C until processing. DNA was extracted with QIAamp DNA blood mini kit, tissue protocol (Qiagen, Germany), according to manufacturer's instructions and stored at -20°C until further processing.

To detect anaplasma or babesial species, screening PCR was performed. For detection of *A. phagocytophilum*, a real-time PCR for the *msp2* gene was performed on all samples (20). Positive samples were further amplified with conventional nested PCR to detect a part of the *ankA* gene of *A. phagocytophilum* (10) and subjected to sequencing to determine the genotype. A conventional PCR with primers PiroA and PiroB that target the hypervariable region of the 18S rRNA gene was used to detect different species of *Babesia* sp. (14). All samples were also tested using a specific conventional PCR with primers for a part of beta-tubulin gene of *B. vulpes* (21). Amplified PCR products of conventional PCRs were separated on gel electrophoresis. All positive samples were purified and sequenced with a BigDye Terminator v3.1 Cycle Sequencing Kit (Applied Biosystems, USA). Sequences obtained were edited using the software CLC Main Workbench 7 (CLCBio, Qiagen, Germany) and compared with sequences available in GenBank.

Results

The DNA of *A. phagocytophilum* was detected in five out of 110 (4.5%) spleen samples from red foxes by real-time PCR for the *msp2* gene, ct values ranged from 23.65 to 28.93 (Table 1). All five samples were subjected to a conventional PCR for a part of *ankA* gene amplification and subsequent sequencing of a PCR product (523 bp). We detected three different sequences that belong to Cluster I (Table 1). One genetic variant (three foxes) had 100% nucleotide identity to a variant that was previously detected in human patients and dogs in Slovenia (acc. No. JQ347533). The second variant (one fox) had 100% nucleotide identity to a

variant detected in a dog in Switzerland (acc. No. KF242674) and Slovenia (not deposited in GenBank). The third genetic variant was 99% similar to a variant detected in a horse from Germany (acc. No. MH973605) but was not previously detected in Slovenia.

Among 110 DNA isolates, 97 (88.2%) were positive with a screening PCR for 18S rRNA gene (377 bp) for *Babesia* sp. Sequencing of PCR product of 18S rRNA gene revealed 80 sequences were identical with each other and to a published sequence of *Babesia vulpes* isolate 03/00349 from a red fox from Spain (Acc. No. KT223483) (Table 1). For 17 PCR products, the nucleotide sequence could not be determined. Therefore, all

samples were subjected to a specific conventional PCR for a part of the beta-tubulin gene of *B. vulpes* (510 bp). Eighty-four (76.3 %) samples were positive and subjected to sequencing. Eighty PCR products were, again, confirmed to be 99% similar to *B. vulpes*. Sequences of four additional PCR products, which previously could not be determined by sequencing of 18S rRNA gene, were now 99% similar to *B. vulpes*. A sequenced part of a beta-tubulin gene from Slovenian red fox babesiae differed from the most similar sequence in a GenBank (*B. microti* isolate SN87-1, fox, USA, AY144707) for one or two nucleotides (99% similarity). *B. vulpes* was detected in samples of red fox from different regions of Slovenia.

Table 1: Detected *A. phagocytophilum* and *B. vulpes* in spleen samples from red fox (*V. vulpes*) in Slovenia

| YEAR OF COLLECTION | REGION | NO. OF SAMPLES | <i>B. vulpes</i> | <i>A. phagocytophilum</i> | |
|--------------------|-------------------------|----------------|-------------------|---------------------------|---|
| | | | positive | positive (ct value) | <i>ankA</i> genotype (Acc. No.) |
| 1996 | Central Slovenia | 1 | 1 | 0 | |
| 1997 | Upper Carniola | 3 | 1 | 1 (27,2) | human, Slovenia (JQ347533) |
| | Central Slovenia | 1 | 1 | 0 | |
| 1998 | Upper Carniola | 2 | 2 | 0 | |
| | Southeast Slovenia | 5 | 5 | 0 | |
| | Central Slovenia | 6 | 4 | 0 | |
| | Lower Sava | 4 | 4 | 1 (26,75) | dog, Switzerland (KF242674) |
| | Littoral-Inner Carniola | 3 | 2 | 0 | |
| | Central Sava | 2 | 2 | 0 | |
| | ND | 6 | 3 | 0 | |
| 1999 | Upper Carniola | 1 | 1 | 0 | |
| 2000 | Upper Carniola | 5 | 2 | 0 | |
| 2002 | Upper Carniola | 2 | 2 | 0 | |
| | Southeast Slovenia | 6 | 5 | 0 | |
| | Central Slovenia | 18 | 16 | 1 (27,38) 1 (28,93) | human, Slovenia (JQ347533) horse, Germany (MH973605) |
| | Savinja | 1 | 1 | 0 | |
| | Central Sava | 1 | 0 | 1 (23,65) | human, Slovenia (JQ347533) |
| 2003 | Upper Carniola | 1 | 1 | 0 | |
| | Southeast Slovenia | 10 | 6 | 0 | |
| | Central Slovenia | 3 | 3 | 0 | |
| | Central Sava | 1 | 0 | 0 | |
| ND | Upper Carniola | 1 | 1 | 0 | |
| | Southeast Slovenia | 5 | 2 | 0 | |
| | Central Slovenia | 11 | 10 | 0 | |
| | Mura | 2 | 1 | 0 | |
| | Littoral-Inner Carniola | 1 | 1 | 0 | |
| | ND | 8 | 7 | 0 | |
| TOTAL | | 110 | 84 (76,3%) | 5 (4,5%) | |



Figure 1: Statistical regions of Slovenia (https://en.wikipedia.org/wiki/Statistical_regions_of_Slovenia)

Discussion

The red fox is an animal species that lives in distinct ecosystems and frequently enters human settings. Consequently, it serves as a possible source of numerous vector-borne pathogens for humans and domestic animals. It has been proven that red fox serves as a species infected with genotypes of *A. phagocytophilum* that are zoonotic (9). Slovenian foxes also harbour genotypes that are pathogenic for humans and dogs, in addition to a newly detected genotype that has been detected before in a German horse. Previously, it has been proposed that wild boars might serve as a reservoir for a human pathogenic strain of *A. phagocytophilum* in Slovenia. Although wild boars are now also entering urbanized areas, red foxes are already adapted to living there. Therefore, a red fox might be the wild species that could serve as a carrier of zoonotic strains of *A. phagocytophilum* to human settings. Although only 4.5% of the samples were detected positive in this study, a rather low number of samples were tested during

each year. The prevalence in foxes may be low, but this species could be a reservoir of pathogens and thus an important source of infection. The infection rate of foxes in Slovenia is in concordance with other European countries (0.8–16.6%) (1). Due to this low infection rate, the red fox may have only limited impact on the circulation of zoonotic genotypes of *A. phagocytophilum* in periurban and urban areas.

According to reports from various countries, *B. vulpes* is prevalent in European countries (14.5–69.2%) (3, 22–27), in North America (37%) (6) and Canada (28). Slovenia is one of the countries with the highest prevalence (75.5%), comparable with reports from NW Spain (Galicia, 72.2%) and from Portugal (69.2%) (24, 29), respectively. Differences in the prevalence among countries might be due to different samples tested or due to different PCR assay used, but also due to different vector species present. In NW Spain and Portugal, the tick *Ixodes hexagonus* is most abundant and was proposed as a vector species (30). In contrast, *B. vulpes* was also discovered in North America, where

I. hexagonus is not endemic (6). It was suggested that *I. ricinus* also might be a vector species for *T. annae*, along with *I. canisuga* (26). The role of non-vector-borne transmission has been suggested, as this is one of the primary routes of transmission for babesiosis in dogs in America (21). Barash et al. found a high prevalence of *B. vulpes* in American Staffordshire and Pit Bull Terrier type dogs that were rescued from dog fighting (21).

Due to the high prevalence of infected red foxes in all regions of Slovenia and due to the fact the red fox frequently enters human settings, this carnivore species poses a threat to domestic dogs. Therefore, veterinarians should be aware of possible infection of a dog with *B. vulpes* as this parasite belongs to the small babesiae group.

Conclusions

Red foxes are infected with a tick-borne zoonotic genotype of *A. phagocytophilum* in Slovenia. Due to its low prevalence, a fox could have only limited impact on the circulation of genotypes pathogenic to human and domestic animals. The prevalence of infection with *B. vulpes* in red foxes in Slovenia is high. That said, red foxes pose a threat to dogs with transmitting this vector-borne pathogen near human settings through the vector of ticks or bites. Veterinarians should be aware of possible small-babesiae infections.

Acknowledgments

The study was supported by the Ministry of Higher Education, Science and Sport of Slovenia (grant no. P3-0083).

We are thankful to Tadej Malovrh for collecting samples, Tina Gabrovšek, Žan Razpotnik and Samo Zakotnik for technical assistance.

References

1. André MR. Diversity of *Anaplasma* and *Ehrlichia/Neoehrlichia* agents in terrestrial wild carnivores worldwide: implications for human and domestic animal health and wildlife conservation. *Front Vet Sci* 2018; 5: e293. DOI: 10.3389/fvets.2018.00293
2. Bateman PW, Fleming PA. Big city life: carnivores in urban environments. *J Zool* 2012; 287: 1–23. DOI:10.1111/j.1469-7998.2011.00887.x
3. Hodžić A, Alić A, Fuehrer HP, et al. A molecular survey of vector-borne pathogens in red foxes (*Vulpes vulpes*) from Bosnia and Herzegovina. *Parasit Vectors* 2015; 8: e88. DOI: 10.1186/s13071-015-0692-x
4. Battisti E, Zanet S, Khalili S, et al. Molecular survey on vector-borne pathogens in Alpine wild carnivores. *Front Vet Sci* 2020; 7: e1. DOI: 10.3389/fvets.2020.00001
5. Szewczyk T, Werszko J, Myczka AW, et al. Molecular detection of *Anaplasma phagocytophilum* in wild carnivores in north-eastern Poland. *Parasit Vectors* 2019; 12(1): e465. DOI: 10.1186/s13071-019-3734-y
6. Birkenheuer AJ, Horney B, Bailey M, et al. *Babesia microti*-like infections are prevalent in North American foxes. *Vet Parasit* 2010; 172: 179–82. DOI: 10.1016/j.vetpar.2010.05.020
7. Gerrikagoitia X, Gil H, García-Esteban C, et al. Presence of *Bartonella* species in wild carnivores of northern Spain. *Appl Environ Microbiol* 2012; 78(3): 885–8. DOI: 10.1128/AEM.05938-11
8. Huhn C, Winter C, Wolfsperger T, et al. Analysis of the population structure of *Anaplasma phagocytophilum* using multilocus sequence typing. *PLOS One* 2013; 9: e4. DOI: 10.1371/journal.pone.0093725
9. Härtwig V, von Loewenich FD, Schulze C, et al. Detection of *Anaplasma phagocytophilum* in red foxes (*Vulpes vulpes*) and raccoon dogs (*Nyctereutes procyonoides*) from Brandenburg, Germany. *Ticks Tick Borne Dis* 2014; 5(3): 277–80. DOI: 10.1016/j.ttbdis.2013.11.001
10. Strašek Smrdel K, von Loewenich FD, Petrovec M, et al. Diversity of *ankA* and *msp4* genes of *Anaplasma phagocytophilum* in Slovenia. *Ticks Tick Borne Dis* 2015; 6(2): 164–6. DOI: 10.1016/j.ttbdis.2014.11.008
11. Strasek Smrdel K, Bidovec A, Malovrh T, et al. Detection of *Anaplasma phagocytophilum* in wild boar in Slovenia. *Clin Microbiol Infect* 2009; 15(Suppl. 2): 50–2. doi: 10.1111/j.1469-0691.2008.02174.x
12. Jalovecka M, Hajdusek O, Sojka D, et al. The complexity of piroplasms life cycles. *Front Cell Infect Microbiol* 2018; 8: e248. DOI: 10.3389/fcimb.2018.00248
13. Duh D, Petrovec M, Avsic-Zupanc T. Molecular characterization of human pathogen *Babesia* EU1 in *Ixodes ricinus* ticks from Slovenia. *J Parasitol* 2005; 91(2): 463–5. DOI: 10.1645/GE-394R

14. Duh D, Petrovec M, Avsic-Zupanc T. Diversity of *Babesia* infecting European sheep ticks (*Ixodes ricinus*). *J Clin Microbiol* 2001; 39(9): 3395–7. doi: 10.1128/jcm.39.9.3395-3397.2001
15. Duh D, Tozon N, Petrovec M, et al. Canine babesiosis in Slovenia: molecular evidence of *Babesia canis canis* and *Babesia canis vogeli*. *Vet Res* 2004; 35(3): 363–8. DOI: 10.1051/vetres:2004018
16. Solano-Gallego L, Sainz A, Roura X, et al. A review of canine babesiosis: the European perspective. *Parasit Vectors* 2016; 9(1): e336. doi: 10.1186/s13071-016-1596-0
17. Harris DJ. Naming no names: comments on the taxonomy of small piroplasmids in canids. *Parasit Vectors* 2016; 9(1): e289. DOI: 10.1186/s13071-016-1567-5
18. Baneth G, Florin-Christensen M, Cardoso L, et al. Reclassification of *Theileria annae* as *Babesia vulpes* sp. nov. *Parasit Vectors* 2015; 8: e207. DOI: 10.1186/s13071-015-0830-5
19. Beck R, Vojta L, Mrljak V, et al. Diversity of *Babesia* and *Theileria* species in symptomatic and asymptomatic dogs in Croatia. *Int J Parasitol* 2009; 39(7): 843–8. DOI: 10.1016/j.ijpara.2008.12.005
20. Courtney JW, Kostelnik LM, Zeidner NS, et al. Multiplex real-time PCR for detection of *Anaplasma phagocytophilum* and *Borrelia burgdorferi*. *J Clin Microbiol* 2004; 42(7): 3164–8. DOI: 10.1128/JCM.42.7.3164-3168.2004
21. Barash NR, Thomas B, Birkenheuer AJ, et al. Prevalence of *Babesia* spp. and clinical characteristics of *Babesia vulpes* infections in North American dogs. *J Vet Intern Med* 2019; 33(5): 2075–81. DOI: 10.1111/jvim.15560
22. Duscher GG, Leschnik M, Fuehrer H-P, et al. Wildlife reservoirs for vector-borne canine, feline and zoonotic infections in Austria. *Int J Parasitol Parasites Wildl* 2014; 4(1): 88–96. DOI: 10.1016/j.ijppaw.2014.12.001
23. Ebani VV, Rocchigiani G, Nardoni S, et al. Molecular detection of tick-borne pathogens in wild red foxes (*Vulpes vulpes*) from Central Italy. *Acta Trop* 2017; 172: 197–200. DOI: 10.1016/j.actatropica.2017.05.014
24. Cardoso L, Cortes HCE, Reis A, et al. Prevalence of *Babesia microti*-like infection in red foxes (*Vulpes vulpes*) from Portugal. *Vet Parasitol* 2013; 196(1/2): 90–5. DOI: 10.1016/j.vetpar.2012.12.060
25. Bartley PM, Hamilton C, Wilson C, et al. Detection of *Babesia annae* DNA in lung exudate samples from red foxes (*Vulpes vulpes*) in Great Britain. *Parasit Vector* 2016; 9: e84. DOI: 10.1186/s13071-016-1364-1
26. Najm NA, Meyer-Kayser E, Hoffmann L, et al. A molecular survey of *Babesia* spp. and *Theileria* spp. in red foxes (*Vulpes vulpes*) and their ticks from Thuringia, Germany. *Ticks Tick Borne Dis* 2014; 5(4): 386–91. DOI: 10.1016/j.ttbdis.2014.01.005
27. Miro G, Checa R, Paparini A, et al. *Theileria annae* (syn. *Babesia microti*-like) infection in dogs in NW Spain detected using direct and indirect diagnostic techniques: clinical report of 75 cases. *Parasit Vector* 2015; 8: e217. DOI: 10.1186/s13071-015-0825-2
28. Clancey N, Horney B, Burton S, et al. *Babesia (Theileria) annae* in a red fox (*Vulpes vulpes*) from Prince Edward Island, Canada. *J Wildl Dis* 2010; 46:2: 615–21. DOI: 10.7589/0090-3558-46.2.615
29. Checa R, Lopez-Beceiro AM, Montoya A, et al. *Babesia microti*-like piroplasm (syn. *Babesia vulpes*) infection in red foxes (*Vulpes vulpes*) in NW Spain (Galicia) and its relationship with *Ixodes hexagonus*. *Vet Parasitol* 2018; 252: 22–8. DOI: 10.1016/j.vetpar.2018.01.011
30. Camacho AT, Pallas E, Gestal JJ, et al. *Ixodes hexagonus* is the main candidate as vector of *Theileria annae* in northwest Spain. *Vet Parasitol* 2003; 112(1): 157–63. DOI: 10.1016/s0304-4017(02)00417-x

UGOTAVLJANJE ANAPLAZME (*Anaplasma phagocytophilum*) IN BABEZIJE (*Babesia vulpes*) V VZORCIH VRANIC PRI RDEČIH LISICAH (*Vulpes vulpes*) V SLOVENIJI

K. Strašek Smrdel, T. Avšič

Izveček: Prehajanje divjih živali v urbana okolja omogoča prenos klopno prenosljivih patogenih mikroorganizmov do dovzetnih oseb in živali. Navadna rdeča lisica (*Vulpes vulpes*) pogosto prehaja v okolico bivališč ljudi, prav tako se je že dobro privadila življenju v bližini ljudi. Zaradi svojih življenjskih navad predstavlja možen vir klopno prenosljivih patogenov preko okuženih klopov, lahko tudi preko ugriza živali. 110 vzorcev vranic navadne rdeče lisice smo pregledali na prisotnost genoma bakterije *Anaplasma phagocytophilum* in parazita *Babesia* spp. Pozitivnim vzorce smo nato določili zaporedje DNK in določili genotip *A. phagocytophilum* oz. vrsto babezije, kadar je bilo to mogoče. Pet vzorcev vranic (4.5 %) navadne rdeče lisice je bilo pozitivnih na prisotnost genoma *A. phagocytophilum*. Z določitvijo zaporedja DNK smo določili tri genotipe. Prevalenca okužbe z *B. vulpes* pri slovenskih lisicah je 76.3 %, določili pa smo jo v vseh statističnih regijah Slovenije. Navadna rdeča lisica ima zelo omejen vpliv na kroženje zoonotskega genotipa *A. phagocytophilum*. Kljub temu pa predstavlja verjeten vir prenosa parazita *B. vulpes* v urbana področja in posledično nevarnost za domače živali.

Ključne besede: navadna rdeča lisica; *Vulpes vulpes*; *Anaplasma phagocytophilum*; *Babesia* spp.; *Babesia vulpes*; klopno prenosljivi patogeni mikroorganizmi; psi

COMPARATIVE EVALUATION OF THE KOMODO DRAGON (*Varanus komodoensis*) AND THE GREEN IGUANA (*Iguana iguana*) SKULL BY THREE-DIMENSIONAL COMPUTED TOMOGRAPHIC RECONSTRUCTION

Sara Pérez¹, Mario Encinoso¹, Manuel Morales¹, Alberto Arencibia², Alejandro Suárez-Bonnet³, Eligia González-Rodríguez¹, J. Raduan Jaber^{2*}

¹Instituto Universitario de Investigaciones Biomédicas y Sanitarias (IUIBS), ²Departamento de Morfología, Facultad de Veterinaria, Universidad de Las Palmas de Gran Canaria. Trasmontaña, Arucas, 35413 Las Palmas, Spain, ³Department of Pathobiology, The Royal Veterinary College, University of London, Hertfordshire, AL9 7TA, London, United Kingdom

*Corresponding author, E-mail: joseraduan.jaber@ulpgc.es

Abstract: The purpose of this paper was to do a comparative evaluation of the skull of two species of lizards, the Komodo dragon (*Varanus komodoensis*) and the Green Iguana (*Iguana iguana*), by three-dimensional computed tomographic reconstruction. Images provided by this method give excellent anatomic detail of the skull. Therefore, essential differences in the configuration of the orbit and the lateral bones of the neurocranium were visualized in lateral and dorsal reconstructed images. The images obtained by tridimensional computed tomographic reconstruction can be a valuable diagnostic aid for the clinical evaluation of several head disturbances in lizards.

Key words: computed tomography; 3D reconstruction; anatomy; skull; lizards

Introduction

Reptiles are a peculiar kind of animal characterized by corneous scales that protect them from desiccation (1). This class of animals is divided into four orders: Chelonians, which comprise turtles, tortoises, and terrapins; Crocodylia, whose specimens are alligators and crocodiles; Rhynchocephalia, with tuataras; and Squamate, represented by two suborders: Ophidia (snakes) and Lacertilia (lizards) (2). Some of these species have become very common in recent years as pets, which became a challenge for veterinary

clinicians since they have to overcome the lack of a reference system similar to canine and feline medicine (3). Thus, it is essential to know and understand their anatomy for an adequate diagnosis and treatment of diseases (4,5).

The introduction of modern diagnostic imaging techniques such as x-ray computed tomography (CT) has been an essential support to specialists. It has afforded the chance to study anatomy and apply it in the clinical features of these species (6). Furthermore, compared with conventional radiography, the digital image format of CT results in improved tissue contrast. In addition, manipulation of the greyscale allows optimal visualization of all tissues within the slice. These characteristics are

advantageous to obtain anatomical information about different regions of the animal body. The recent advances in CT technology include applying computer software to generate three-dimensional (3D) construction of an area of anatomic interest. This technique requires multiple thin section images, and the advantages of this process are that anatomical detail is improved, and can image bony structures with different degrees of rotation (6). CT reconstruction has already been used in morphofunctional studies performed in the Savannah monitor (7) and American Alligator (8). However, there are no reports concerning comparative anatomy of the skull of different species of reptiles by three-dimensional reconstructed CT to the author's knowledge. The few descriptions performed in these species only deal with cross-sectional studies such as those done in the Boa constrictor (4), the Green iguana, the Common tegu, and the Bearded dragon head (5), and more recently, an anatomic interactive atlas of the loggerhead sea turtle head using images obtained via osteology, gross dissections, and computed tomography (9). Therefore, this study aimed to describe and compare the normal anatomy of two species of lizards, the Komodo dragon (*Varanus komodoensis*) and Green iguana (*Iguana iguana*) skull performing three-dimensional CT reconstruction.

Materials and methods

Animals

Two adult female Komodo dragons (*Varanus komodoensis*) and two male green iguanas (*Iguana iguana*) were imaged at the Veterinary Clinic Hospital of Las Palmas de Gran Canaria University. No physical examination abnormalities were detected before the study. The reptiles owner was informed of the study and signed consent for participation in it.

CT technique

Sequential transverse CT slices were obtained using a 16-slice helical CT scanner (Toshiba Astelion, Toshiba Medical System, Madrid, Spain). The animals were positioned symmetrically in ventral recumbency on the CT couch. A standard clinical protocol (120 kVp, 80 mA, 512 X 512

acquisition matrix, 1809 x 858 field of view, a spiral pitch factor of 0.94, and a gantry rotation of 1.5 s) was used to acquire sequential transverse CT images of 1 mm thickness slice. The original transverse data were stored and transferred to the CT workstation. No CT density or anatomic variations were detected in the head of the reptiles used in the investigation. In this study, we applied two CT windows by adjusting the window widths (WW) and window levels (WL) to appreciate the CT appearance of the head structures: a bone window setting (WW = 1500; WL = 300) and a soft tissue window setting (WW = 350; WL = 40). The original data were used to generate head volume-rendered reconstructed images after manual editing of the transverse CT images to remove soft tissues using a standard Dicom 3D format (OsiriX MD, Geneva, Switzerland).

Results

Head three-dimensional volume-rendered reconstruction images corresponding to dorsal (Fig. 1, 4) and ventral (Fig. 2, 5) views and the left lateral view (Fig. 3, 6) of the Komodo dragon and green iguana head. Volume-rendered reconstructed CT images showed excellent visualization of the bones that comprised the skull. Therefore, in the Komodo dragon head, the orbit was cranial and ventrally delimited by the lacrimal, the prefrontal, and the jugal bones (Figs. 1,3). Besides, this technique allowed us to visualize the relation between this last and the ectopterygoid bone (Fig.3). Caudodorsally, the junction of the postorbital and postfrontal bones could be observed in the lateral and dorsal reconstructed CT images (Figs. 1,3). Moreover, the ventral CT reconstructed image identified the intersection of the frontal and the parietal bones. The different bones of the neurocranium, such as the parabasisphenoid, the basioccipital, and the prootic bones, were easily identifiable (Fig. 2). Besides, the laminar disposition of the vomer and how it supports the septomaxilla were observed (Fig.2). The junction between the premaxilla and the maxilla with the tooth arranged in a straight row was identified in the lateral and ventral reconstructed CT images (Figs. 2,3). The jaw showed a straight tooth row and a curved ventral border in the lateral reconstructed CT image. In addition, the coronoid process was quite prominent, and the surangu-

lar and articular bones were observed extending caudally (Fig. 3). The ventral reconstructed image showed excellent pterygoid visualization, which is flat and “y” shaped bone. This one had a rounded process, where the caudal border of the

palatine process contacts. This view also depicted the junction between the parabasisphenoid, the prootic, and the basioccipital bones. The ventral portion of this last bone constituted the occipital condyle (Fig. 2).

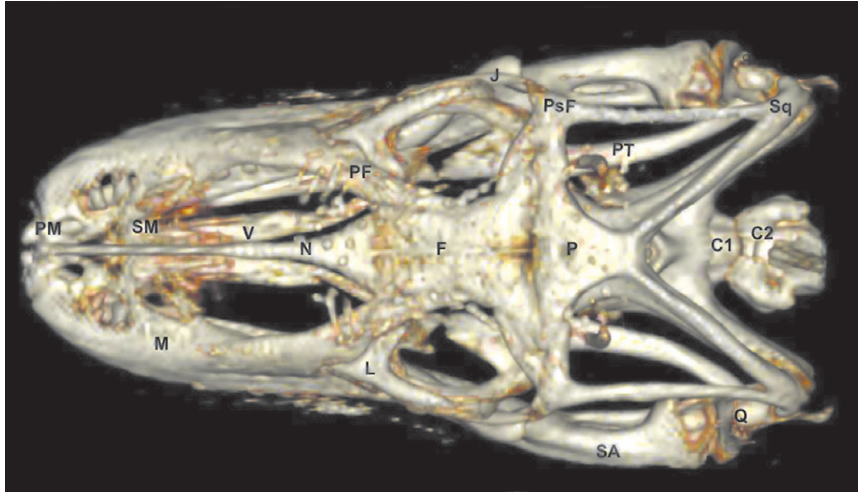


Figure 1: Three-dimensional volume-rendered reconstruction image of the normal Komodo dragon head. Dorsal aspect. PM: Premaxillary bone. M: Maxillary bone. SM: Septomaxilla. N: Nasal bone. V: Vomer. PF: Prefrontal bone. F: Frontal bone. L: Lacrimal bone. J: Jugal bone. Q: Quadrate bone. Sq: Squamosal. PsF: Postfrontal+postorbital. P: Parietal. PT: Pterygoid bone. SA: Surangular bone. C1: First cervical vertebra. C2: Second cervical vertebra

Figure 2: Three-dimensional volume-rendered reconstruction image of the normal Komodo dragon head. Ventral aspect. D: Dentary bone. SA: Surangular bone. A: Articular bone. SM: Septomaxilla. V: Vomer. PL: Palatine bone. PT: Pterygoid bone. PsF: Postfrontal+postorbital bone. N: Nasal bone. F: Frontal bone. P: Parietal bone. PB: Parabasisphenoid bone. BO: Basioccipital bone. OC: Occipital condyle. PRO: Prootic bone. Q: Quadrate bone.

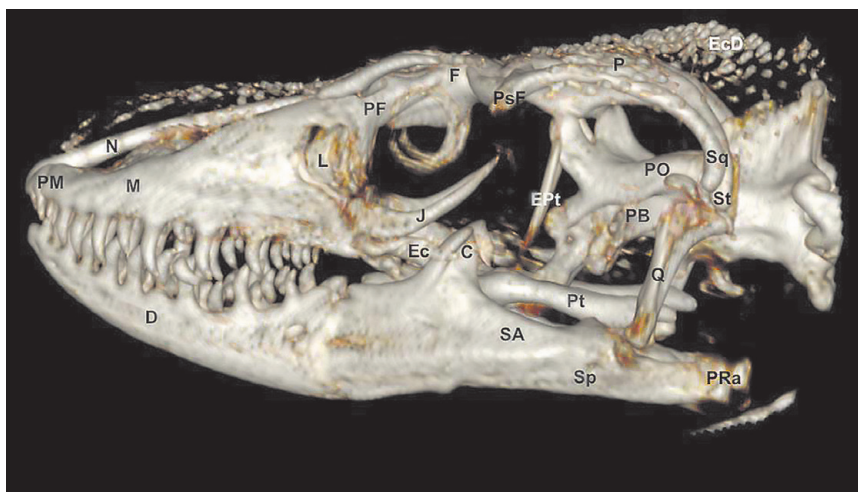
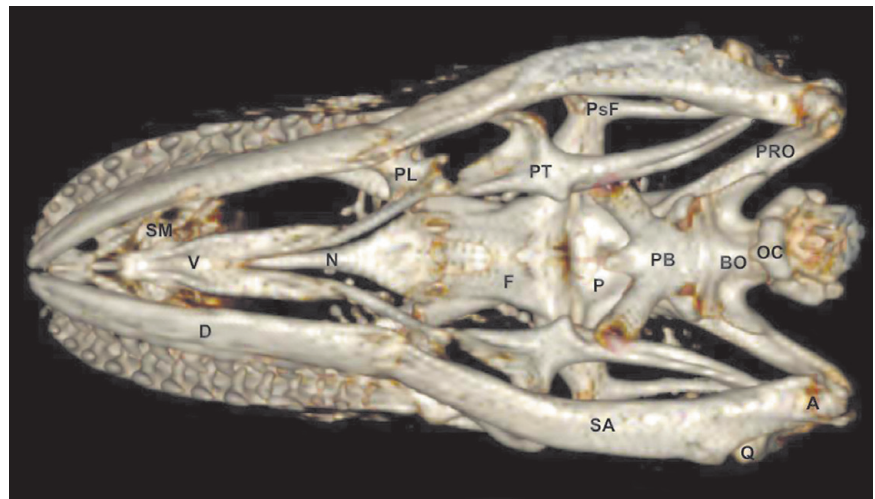


Figure 3: Three-dimensional volume-rendered reconstruction image of the normal Komodo dragon head. Lateral aspect. PM: Premaxillary bone. M: Maxillary bone. PF: Prefrontal bone. N: Nasal bone. F: Frontal bone. L: Lacrimal bone. J: Jugal bone. Ec: Ectopterygoid bone. Pt: Pterygoid bone. Ept: Epipterygoid. Q: Quadrate bone. St: Supratemporal. Sq: Squamosal. PsF: Postfrontal+postorbital. PRO: Prootic. PB: Parabasisphenoid bone. P: Parietalbone. D: Dentary bone. C: Coronoid bone. SA: Surangular bone. Sp: Splenic. PRa: Retroarticular process. EcD: Osteoderms

Concerning the green iguana head, the lateral reconstructed images showed a high and domed skull (Fig. 6). In contrast with the Komodo dragon head, the orbit of the green iguana was closed by the postfrontal and the postorbital bone junction, which was extended to the posterior margins of bony orbits till articulate with the jugal bone (Figs. 4,6). Therefore, the jugal formed the lateral wall of the bony orbit and was joined with lacrimal (dorsally), maxillary (ventrally), ectopterygoid (medially), postorbital (caudodorsally), and squamosal (caudally) (Fig. 6). This view identified frontal, parietal, and postfrontal bones (Fig. 6). Moreover, the prefrontal bones connecting rostrally maxillary and nasal bones, laterally to lacrimal bones, and caudodorsally to frontal bones were also identified in the dorsal view (Fig. 4). This prefrontal bone participated in the dorsal and rostral orbit walls (Figs. 4,6). This lateral view showed the junction between squamosal, ectopterygoid, epipterygoid, pterygoid, quadrate, and prootic bones. This last one had a square shape and formed the neurocranium's lateral walls, which were also well visualized in ventral reconstructed images (Fig. 5). Thus, the junction between the basioccipital, the parabasisphenoid bones, and its lateral connection with the pterygoid could be observed. These ventral and lateral reconstructed images showed the bones composing the jaw. Thus, the dentary, the coronoid, the surangular, and the articular bones were evident in these views.

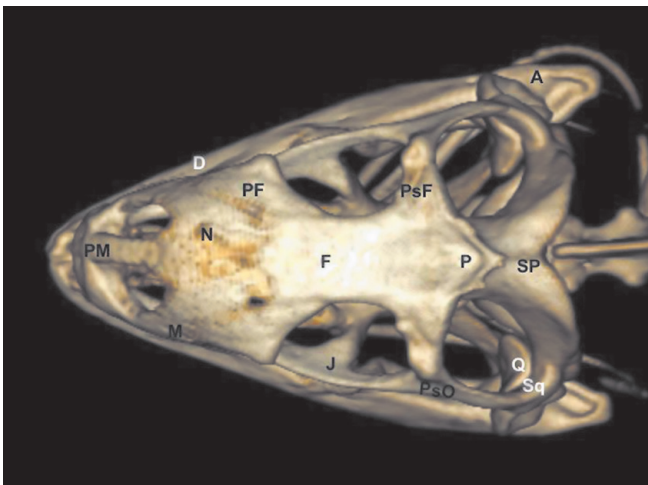


Figure 4: Three-dimensional volume-rendered reconstruction image of the normal Green iguana head. Dorsal aspect. PM: Preamaxillary bone. M: Maxillary bone. N: Nasal bone. PF: Prefrontal bone. F: Frontal bone. J: Jugal bone. Q: Quadrate bone. Sq: Squamosal. PsF: Postfrontal. PsO: Postorbital. P: Parietal. SP: Supraoccipital bone. D: Dentary bone. A: Articular bone

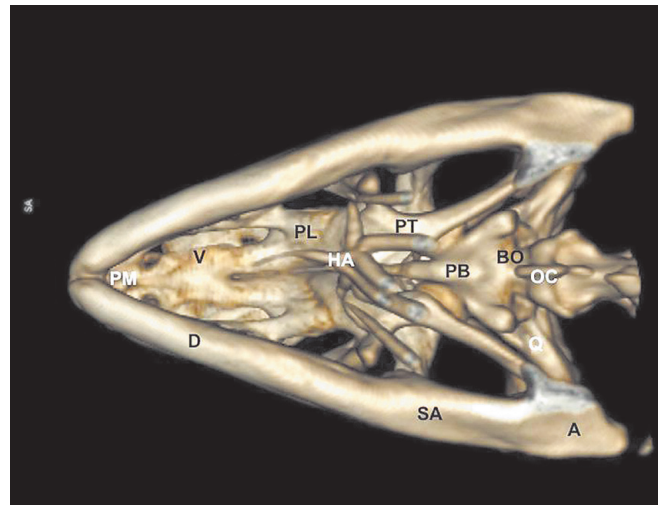


Figure 5: Three-dimensional volume-rendered reconstruction image of the normal Green iguana head. Ventral aspect. D: Dentary bone. SA: Surangular bone. A: Articular bone. PM: Preamaxillary bone. V: Vomer. PL: Palatine bone. PT: Pterygoid bone. PB: Parabasisphenoid bone. BO: Basioccipital bone. Q: Quadrate bone. OC: Occipital condyle. HA: Hyoid apparatus

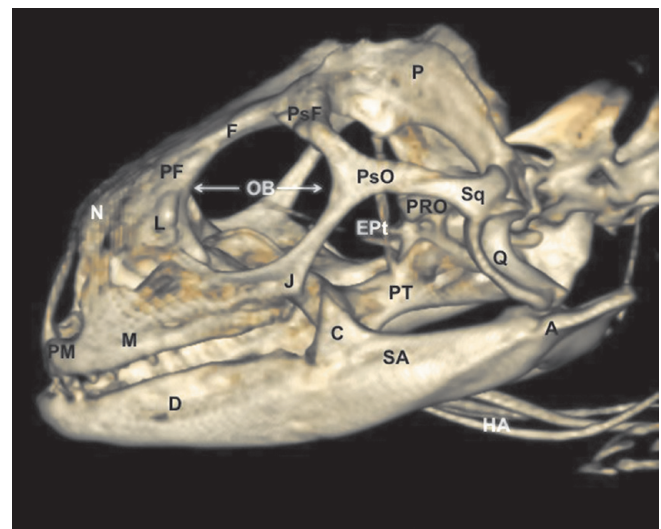


Figure 6: Three-dimensional volume-rendered reconstruction image of the normal Green iguana head. Lateral aspect. PM: Preamaxillary bone. M: Maxillary bone. PF: Prefrontal bone. N: Nasal bone. F: Frontal bone. OB: Orbit. L: Lacrimal bone. J: Jugal bone. PsF: Postfrontal bone. PsO: postorbital bone. PT: Pterygoid bone. EPT: Epipterygoid. Q: Quadrate bone. Sq: Squamosal. PRO: Prootic. P: Parietal bone. D: Dentary bone. C: Coronoid bone. SA: Surangular bone. A: Articular bone. HA: Hyoid apparatus

Discussion

The arrival of imaging techniques to reptile medicine has improved veterinary medicine diagnosis (5-9). Traditionally, radiography (10)

and ultrasonography (11) have been applied to obtain information on the bony and the main soft-tissue structures of different animal regions. In contrast, computed tomography has become the preferred imaging technique due to its considerable advantages (11). Hence, last-generation CT equipment gives fast imaging acquisition, body sections from different tomographic planes, fair anatomic resolution without superimposition, and excellent tissue-like differentiation (5,9).

Three-dimensional CT reconstruction is a valuable procedure, which is infrequently applied in veterinary medicine. The data collection requires multiple parallel thin sections, which are all obtained at the same gantry tilt. Ideally, a high-speed scanner such as the scanning beam 'cine' CT system can produce a rapid sequence of quality thin sections to minimize motion artifact (12). This procedure can image the surface of bony structures with different degrees of rotation without the superimposition of soft tissues (12,13,14).

As in other lizards, the Komodo dragon and the Green Iguana skull are complex structures composed of different bones with significant disparity. However, in contrast with other reports that did radiographs (4,5), the use of reconstructed images of the skull avoided the superimposing of the bilateral structures of the snout and neurocranium to give excellent visualization of the junction between bones that comprise the head. Thus, lateral and dorsal reconstructed images visualized essential differences between the species studied. Therefore, an enormous difference in the orbit composition was observed in the species studied, especially along the posterior margin of the orbit, where it was closed (Green iguana) or open (Komodo dragon). This fact was determined by variations in the shape, size, and presence of the jugal bone and variations in the postorbital and postfrontal bones, as explained by Daza and Bauer (15). Besides, in the lateral side of the neurocranium could be identified the prootic bone, which had a square shape in the Green iguana. In contrast, it was tubular in the Komodo dragon.

Other investigations have studied the comparative and morphometrics features of the skull in terrestrial mammals by three-dimensional computed tomographic reconstruction (16). Nonetheless, in our study, anatomical measurements of the head and mandible were not performed since

the number of specimens studied was scarce to perform statistical analysis.

In conclusion, we have attempted to describe our findings on recognizable structures in alive reptiles, but further studies are necessary to define the ultimate limits of 3D CT reconstruction for essential morphologic imaging and interpretation of animals with clinical signs. Nevertheless, the CT reconstructed images obtained in this study facilitated an adequate anatomical understanding of the Komodo dragon and Green iguana skull. This information could be used to diagnose disorders involving the head of lizards, such as metabolic bone diseases, fractures, and neoplasias.

Acknowledgment

In loving memory of Alvaro Domingo Rodriguez Garcia. We also thank Marisa Mohamad for her support and constructive comments.

Authors declare that no any conflict of interest exists.

References

1. Gumpenberger M. Diagnostic imaging of reproductive tract disorders in reptiles. *Vet Clin North Am Exot Anim Pract* 2017; 20(2): 327–43.
2. Hernández C, Peloso PL, Bolívar W, Daza JD. Skull morphology of the lizard *PtychoGLOSSUS vallensis* (Squamata:Alopoglossidae) with comments on the variation within Gymnophthalmoidea. *Anat Rec* 2019; 302(7): 1074–92.
3. Banzato T, Hellebuyck T, Van Caelenberg A, Saunders JH, Zotti A. A review of diagnostic imaging of snakes and lizards. *Vet Rec* 2013; 173(2): 439.
4. Banzato T, Russo E, Di Toma A, Palmisano G, Zotti A. Anatomic imaging of the Boa constrictor head: a comparison between radiography, computed tomography and cadaver anatomy. *Am J Vet Res* 2011; 72(12): 1592–9.
5. Banzato T, Selleri P, Veladiano IA, Martin A, Zanetti E, Zotti A. Comparative evaluation of the cadaveric, radiographic and computed tomographic anatomy of the heads of green iguana (*Iguana iguana*), common tegu (*Tupinambis merianae*) and bearded dragon (*Pogona vitticeps*). *BMC Vet Res* 2012; 8: e53. doi: 10.1186/1746-6148-8-53
6. Lauridsen H, Hansen K, Wang T, et al. Inside out: modern imaging techniques to reveal

animal anatomy. PLoS ONE 2011; 6(3): e17879. doi: 10.1371/journal.pone.0017879

7. Wilken AT, Middleton KM, Sellers KC, Cost IN, Holliday CM. The roles of joint tissues and jaw muscles in palatal biomechanics of the savannah monitor (*Varanus exanthematicus*) and their significance for cranial kinesis. J Exp Biol 2019; 222 (Pt 18): jeb201459.

8. Holliday CM, Tsai HP, Skiljan RJ, George ID, Pathan S. A 3D iInteractive model and atlas of the jaw musculature of *Alligator mississippiensis*. PLoS One 2013; 8(6): e62806. doi: 10.1371/journal.pone.0062806

9. Arencibia A, Melian A, Oros J. Anatomic interactive atlas of the loggerhead sea turtle (*Caretta caretta*) head. Animals 2021; 11(1): e198. doi: 10.3390/ani11010198

10. Knipe FM. Principles of neurological imaging of exotic animal species. Vet Clin North Am Exot Anim Pract 2007; 10(3): 893–907.

11. Krautwald-Junghanns ME, Pees M, Reese S. Diagnostic imaging of exotic pets. Hannover : Schlutersche, 2011: 310–459.

12. Arencibia A, Corbera JA, Ramírez G, et al. Anatomical assessment of the thorax in the neonatal foal using computed tomography angiography, sectional anatomy and gross dissections. Animals 2020; 10(6): e1045. doi: 10.3390/ani10061045

13. Zafra R, Carrascosa C, Suarez-Bonnet A, et al. Three-dimensional reconstruction by computed tomography of an undifferentiated sarcoma in a dog. J Appl Anim Res 2012; 40(4): 289–91.

14. Jaber JR, Carrascosa C, Arencibia A, Corbera JA, Ramirez AS, Melian C. 3-D computed tomography reconstruction: another tool to teach anatomy in the veterinary colleges. Iran J Vet Res 2018; 19(1): 1-2.

15. Daza JD, Bauer AM. The circumorbital bones of the Gekkota (Reptilia: Squamata). Anat Rec 2010; 293(3): 402–13.

16. Moselhy AA, Mahdy, E. Comparative three dimensional computed tomography (CT) scans and anatomical investigation of rabbit (*Oryctolagus cuniculus*) and cat (*Felis domestica*) skull. Slov Vet Res 2019; 56 (Suppl 22): 365–79.

PRIMERJAVA LOBANJ KOMODOŠKEGA VARANA (*Varanus komodoensis*) IN ZELENEGA LEGVANA (*Iguana iguana*) S POMOČJO TRIDIMENZIONALNE RAČUNALNIŠKE TOMOGRAFSKE REKONSTRUKCIJE

S. Pérez, M. Encinosa, M. Morales, A. Arencibia, A. Suárez-Bonnet, E. González-Rodríguez, J. R. Jaber

Izvleček: Namen prispevka je bil s tridimenzionalno računalniško tomografsko rekonstrukcijo opraviti primerjalno oceno lobanje dveh vrst kuščarjev, komodoškega varana (*Varanus komodoensis*) in zelenega legvana (*Iguana iguana*). Slike, pridobljene s to metodo, prikažejo odlične anatomske podrobnosti lobanje. Zato so bile na stranskih in dorzalnih rekonstrukcijah slik vidne bistvene razlike v zgradbi orbitalnega področja in stranskih kosti nevrokranija med obema vrstama kuščarjev. Slike, pridobljene s tridimenzionalno računalniško tomografsko rekonstrukcijo, so lahko dragocena diagnostična pomoč pri klinični oceni večih napak glave pri kuščarjih.

Ključne besede: računalniška tomografija; 3D rekonstrukcija; anatomija; lobanja; kuščarji

OSTEOMYELITIS ON THE CERVICAL VERTEBRAS OF A FREE-LIVING EUROPEAN HEDGEHOG (*Erinaceus europaeus*) BY *Paeniclostridium sordellii*

Andreia Garcês^{1*}, Vanessa Soeiro², Sara Lóio², Filipe Silva^{3,4}, Isabel Pires^{3,4}

¹Inno – Serviços Especializados em Veterinária, R. Cândido de Sousa 15, 4710-300 Braga, Portugal, ²Wildlife Rehabilitation Centre of Parque Biológico de Gaia, Rua da Cunha, 152, Avintes, ³Veterinary Science Department, ⁴CECAV, University of Trás-os-Montes and Alto Douro, 5000-801, Vila Real, Portugal

*Corresponding author, E-mail: andreamvg@gmail.com

Abstract: A free-living European hedgehog (*Erinaceus europaeus*) adult female was admitted to the Wildlife Rehabilitation Centre of Parque Biológico de Gaia (Portugal), with severe breathing distress and poor body condition. Its neck was displaced 60 degrees caudally. During the *post-mortem* exam, an abscess in the cervical vertebrae was observed. *Paeniclostridium sordellii* was the agent isolated from the purulent exudate that was removed from the lesion. This is the first reported case of *P. sordellii* associated osteomyelitis on the cervical vertebrae, and the first time that this pathology is described in this species associated with this agent.

Key words: *Erinaceus europaeus*; Portugal; *Paeniclostridium sordellii*; osteomyelitis

Introduction

The Western European hedgehog *Erinaceus europaeus* (Linnaeus, 1758) is a generalist mammal, widely distributed by the European continent (1–3). Highly adaptable animals that can be frequently observed in green spaces in constructed-up areas such as gardens and parks in the cities (4,5). Hedgehogs are one of the most common species admitted to wildlife rehabilitation centres or veterinary hospital, but still little is known about their diseases and agents (5,6).

Usually, cervical osteomyelitis occurs in very old individuals or young animals with active

growth plates, associated with *Staphylococci spp* and *Escherichia coli* infection (7). In hedgehogs cases of maxillary osteomyelitis had already been reported (8).

Paeniclostridium sordellii (previously *Clostridium sordellii*) is a gram-positive, sporulating anaerobic rod that is a common inhabitant of soil, and very rarely can be found in the intestinal content of clinically healthy animals. It can invade wounds and tissues pre and post mortem. It has been associated with enteric disease of several animal species, but still remains controversial (9–11) including several clostridial species. *P. sordellii* is also responsible for fatal toxic shock and bacteraemia in humans (10).

An adult female of European hedgehog (*E. europaeus*) weighing 560 g was admitted to the Wildlife Rehabilitation Centre of Parque Biológico de Gaia (Portugal), after being found during the day in a suburban area, with prostration and respiratory difficulties. On examination, the

animal had a poor body condition, weakness of the limbs, pallid mucosa's, respiratory distress, an abnormal position of the neck and dehydration. Its neck was displaced 60 degrees caudally, as observed in Figure 1A. Unfortunately, the animal died during the treatment.

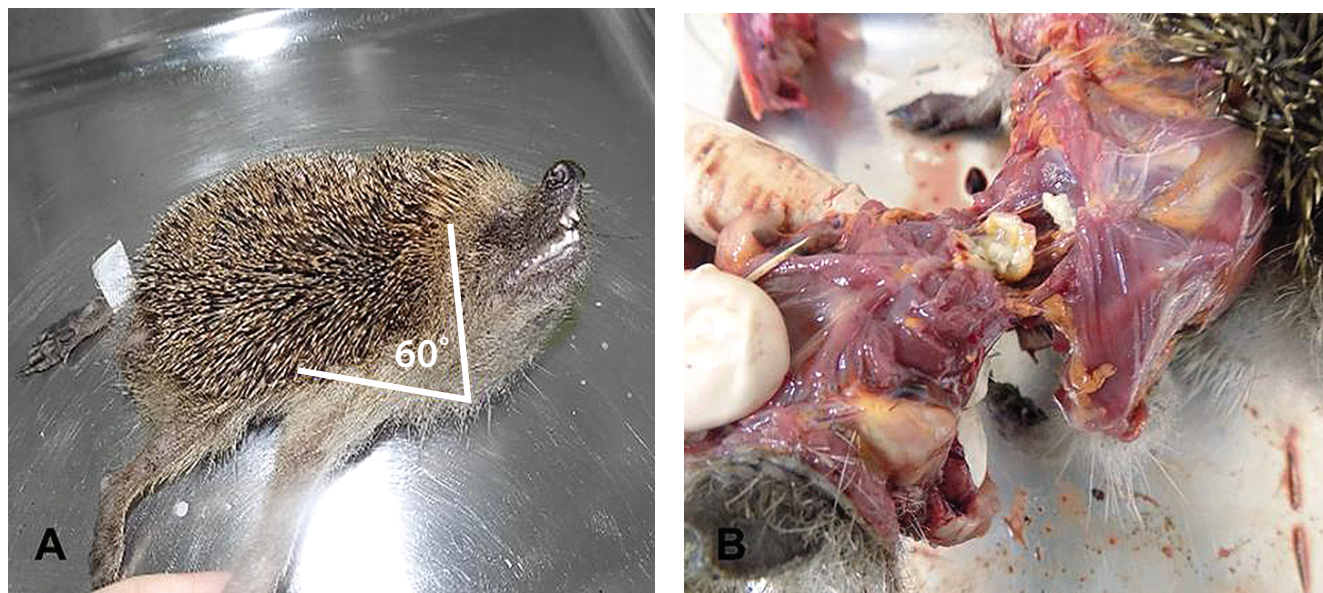


Figure 1: A *Erinaceus europaeus* with the neck pushed in 60 degrees caudally. In B encapsulated nodule with 1cm in diameter, filled with a whitish purulent exudate, on the C2-C3 vertebrae

On the *post-mortem* examination, an encapsulated nodule with 1cm in diameter, filled with a whitish purulent exudate, was observed adjacent to the C2-C3 vertebrae. The consistence was fresh cheese-like (Figure 1B) and the pus invaded C2 and C3 vertebrae, that also presented osteolysis. The lungs presented congestion and oedema. There was an absence of food content in the stomach that contained mucus. The urinary bladder was distended with urine. No more gross lesions were detected.

An impression smear of the nodule was performed and gram-positive bacteria (rods) and neutrophils (some degenerated) were observed. Representative tissues specimens were collected for histologic examination (12). Histopathology of the vertebrae was not possible due to the extensive osteolysis which caused fragmentation of the material. Other microscopic findings included parasitic interstitial pneumonia and multifocal hepatitis. The purulent material was also submitted to microbiological analysis. The agent *Paenibacillus sordellii* was identified using VITEK® system (ANC ID Car REF 21347, Biomérieux, France), after the grown in anaerobioses of small

colonies with 1-4 mm in diameter that spread on the plate in a continuous firm, with a translucent coloration on the Blood BHI, for 24h at 35-37° C.

Discussion and conclusion

Although maxillary osteomyelitis had already been reported in *E. europaeus* (8), it is the first time that a cervical osteomyelitis is reported in this specie.

In this particular case, the diagnosis was only made during the *post-mortem* exam because it was not possible to perform any complementary diagnostic exams (e. g. radiography) before the animal die. After death has not possible to perform radiographic exams due to limitations on the resources.

The clinical signs that the animal presented could be associated not only to the deformation of the spine and compression of the spinal cord but also associated with the toxic effects of the bacteria. The port of entry for bacteria could have been a small skin wound that had already healed at the time of clinical presentation but

was not possible to collect tissue of those areas to posterior histopathology exam. Since *E. europaeus* have scavengers behaviours, live close to the ground and even in underground holes, and this pathogenic agent is common in soils, is possible that have invade a *premortem* wound leading to the development of the abscess. Local proliferation of the agent may had occurred, and the suppurate exudate formed may have extended by contiguity to the adjacent vertebrae. There are only a few reports of osteomyelitis in cervical vertebrae in wild mammals (13), and this case report for the first time a cervical osteomyelitis in a wild *E. europaeus*.

In veterinary *P. sordellii* has an important role particular in farm animals, having been associated to gas gangrene in ruminants, pigs, and horses, ulcerative enteritis in quail, abomasitis in lambs, necrotic enteritis in chickens, omphalitis in foals, and other enteric infections in wild species (e.g. bears, pelicans) (9). But it is the first time that *P. sordellii* is associated to an osteomyelitis.

Reports as this are import not only to improve the knowledge on disease in that *E. europaeus*, but also in other domestic and non-domestic species, including humans, since this agent has the potential of becoming zoonotic.

Acknowledgements

We are grateful to Parque Biológico de Gaia, Laboratory of Histology and Anatomic Pathology of UTAD and INNO Veterinary Laboratory for the support in the execution of this work.

The author(s) declare that there are no conflicts of interest. This research did not receive any specific grant from funding agencies in the public, commercial, or not-for-profit sectors.

No ethical approval was obtained because this study did not involve a prospective evaluation and did not involve laboratory animals. Informed consent for publication of clinical information's and images was obtained from the Wildlife Rehabilitation Centre of Parque Biológico de Gaia and from the ICNF (Instituto da Conservação da Natureza e das Florestas).

References

1. Reeve N. Hedgehogs. London : Poyser, 2002: 304 p.
2. Mullineaux E, Best D, Cooper JE. BSAVA manual of wildlife casualties. Gloucester : British Small Animal Veterinary Association, 2003.
3. Pettett CE, Moorhouse TP, Johnson PJ, Macdonald DW. Factors affecting hedgehog (*Erinaceus europaeus*) attraction to rural villages in arable landscapes. Eur J Wildl Res 2017; 63(3): art. 54.
4. Rasmussen SL, Berg TB, Dabelsteen T, Jones OR. The ecology of suburban juvenile European hedgehogs (*Erinaceus europaeus*) in Denmark. Ecol Evol 2019; 9(23): 13174–87.
5. Bexton S. Hedgehogs. In: Mullineaux E, Keeble E, eds. BSAVA manual of wildlife casualties. 2nd ed. Gloucester : British Small Animal Veterinary Association, 2016: 117–37.
6. Martínez J, Rosique, Alejandro I, Royo M. Causes of admission and final dispositions of hedgehogs admitted to three Wildlife Rehabilitation Centers in eastern Spain. Hystrix 2014; 25(2): 107–10.
7. Maier K, Fischer D, Hartmann A, et al. Vertebral osteomyelitis and septic arthritis associated with *Staphylococcus hyicus* in a juvenile peregrine falcon (*Falco peregrinus*). J Avian Med Surg 2015; 29(3): 216–23.
8. Martínez LS, Juan-Sallés C, Cucchi-Stefanoni K, Garner MM. *Actinomyces naeslundii* infection in an African hedgehog (*Atelerix albiventris*) with mandibular osteomyelitis and cellulitis. Vet Rec 2005; 157(15): 450–1.
9. Nyaoke AC, Navarro MA, Fresneda K, et al. *Paeniclostridium (Clostridium) sordellii*-associated enterocolitis in 7 horses. J Vet Diagn Invest 2020; 32(2): 239–45.
10. Rabi R, Turnbull L, Whitchurch C, Awad M, Lyras D. Structural characterization of *Clostridium sordellii* spores of diverse human, animal, and environmental origin and comparison to *Clostridium difficile* spores. mSphere. 2017; 2(5): e00343–17. doi: 10.1128/mSphere.00343-17
11. Sasi Jyothsna TS, Tushar L, Sasikala C, Ramana CV. *Paraclostridium benzoelyticum* gen. nov., sp. nov., isolated from marine sediment and reclassification of *Clostridium bifermentans* as *Paraclostridium bifermentans* comb. nov. Proposal of a new genus *Paeniclostridium* gen. nov. to accommodate *Clostridium sord.* Int J Syst Evol Microbiol 2016; 66(3): 1268–74.
12. Mescher AL. Junqueira's basic histology: text and atlas. 13th ed. New York : McGraw-Hill Education, 2013.
13. Raymond JT, White MR. Necropsy and histopathologic findings in 14 African hedgehogs (*Atelerix albiventris*): a retrospective study. J Zoo Wildl Med 1999; 30(2): 273–7.

OSTEOMIELITIS VRATNIH VRETENC PRI PROSTOŽIVEČM EVROPSKEM JEŽU (*Erinaceus europaeus*), POVZROČEN Z BAKTERIJO *Paeniclostridium sordellii*

A. Garcês, V. Soeiro, S. Lóio, F. Silva, I. Pires

Izveček: Prosto živeča odrasla samica evropskega ježa (*Erinaceus europaeus*) je bila sprejeta v Center za rehabilitacijo divjih živali Parque Biológico de Gaia (Portugalska) s hudo dihalno stisko in slabim telesnim stanjem. Njen vrat je bil premaknjen kavalno za 60 stopinj. Med sekcijo po smrti so opazili absces na vratnih vretencih. Iz gnojnega eksudata lezije je bila izolirana bakterija *Paeniclostridium sordellii*. V članku poročamo o prvem zabeleženem primeru osteomielitisa, povezanega s *P. sordellii*, na vratnih vretencih in o prvem primeru opisa tovrstne patologije pri evropskem ježu, povezani s tem povzročiteljem.

Ključne besede: *Erinaceus europaeus*; Portugalska; *Paeniclostridium sordellii*; osteomielitis

SLOVENIAN VETERINARY RESEARCH SLOVENSKI VETERINARSKI ZBORNIK

Slov Vet Res 2021; 58 (3)

Original Research Articles

- Kandeel M, El-Deeb W, Fayez M, Ghoneim I. Pharmacokinetics of the long-acting ceftiofur crystalline-free acid in Arabian she-camels (*Camelus dromedarius*) 95
- Strašek Smrdel K, Avšič T. The detection of *Anaplasma phagocytophilum* and *Babesia vulpes* in spleen samples of red fox (*Vulpes vulpes*) in Slovenia 103
- Pérez S, Encinosa M, Morales M, Arencibia A, Suárez-Bonnet A, González-Rodríguez E, Jaber JR. Comparative evaluation of the Komodo dragon (*Varanus komodoensis*) and the Green iguana (*Iguana iguana*) skull by three-dimensional computed tomographic reconstruction 111

Case Report

- Garcês A, Soeiro V, Lóio S, Silva F, Pires I. Osteomyelitis on the cervical vertebrae of a free-living European hedgehog (*Erinaceus europaeus*) by *Paenibacillus sordellii* 117